ELSEVIER

Solid State Ionics 111 (1998) 243–252

SOLID STATE IONICS

Effect of mixed solvent electrolytes on cycling performance of rechargeable $Li/LiNi_{0.5}Co_{0.5}O_2$ cells with gel polymer electrolytes

Dong-Won Kim*, Yang-Kook Sun

Polymer Materials Laboratory, Samsung Advanced Institute of Technology, 103-12, Moonji-Dong, Yusung-Gu, Daejon 305-380, Korea

Received 25 February 1998; accepted 1 June 1998

Abstract

New polymer electrolytes based on acrylonitrile-methyl methacrylate-styrene (AMS) terpolymers were prepared using binary plasticizing solvents consisting of ethylene carbonate (EC)/dimethyl carbonate (DMC) or EC/Y-butylolactone (Y-BL). The $LiNi_{0.5}Co_{0.5}O_2$ powders with narrow particle-size distribution and phase-pure particles were also synthesized by a sol-gel method using aspartic acid as a chelating agent. With these solid polymer electrolytes (SPE) and $LiNi_{0.5}Co_{0.5}O_2$ powders, the $Li/SPE/LiNi_{0.5}Co_{0.5}O_2$ cells were assembled and their cycling performance was investigated in terms of mixed solvent electrolytes. The cyclability of $Li/SPE/LiNi_{0.5}Co_{0.5}O_2$ cell was significantly affected by the nature of the solvent. The $Li/SPE/LiNi_{0.5}Co_{0.5}O_2$ cells containing EC/DMC mixture showed better cycling characteristics as compared to those based on EC/Y-BL mixture. These cells had an initial capacity of 156 mAh/g in the voltage range of 3.0–4.2 V, and showed an attractive discharge capacity of 116 mAh/g at 2.0 C rate.

Keywords: Lithium-nickel-cobalt oxide; Lithium polymer battery; Passivation; Polymer electrolyte; Terpolymer

1. Introduction

Lithium polymer batteries are now being widely studied and developed as rechargeable energy sources, the most important of which is for high energy density batteries. However the demands on battery performance have required further improvements in polymer electrolytes. In view of applications, a large amount of work has been carried out to optimize the gel polymer electrolytes in which the liquid electrolyte has been immobilized by incorporation into a matrix polymer, such as polyacrylonitrile (PAN) [1–3], poly(vinylidene fluoride) (PVdF) [4,5], poly(vinyl chloride) (PVC) [6,7] and poly(vinyl pyrrolidone) (PVP) [8]. These plasticized polymer electrolytes combine the best features of both liquid and solid electrolytes. In our group, electrical properties of the plasticized polymer electrolytes based on acrylonitrile-methyl methacrylate copolymer and acrylonitrile-methyl methacrylate-(oligo oxyethylene) ethyl ether methacrylate terpolymer have been reported [9,10]. These studies demonstrated that the use of copolymers for polymer electrolytes allowed us to optimize physico-chemical properties such as ionic conductivity, mechanical properties, compatibility with plasticizing electrolyte solution, and stability towards the lithium electrodes.

*Corresponding author. Tel.: +82-42-865-4074; fax: +82-42-865-4620; e-mail: dwkim@saitgw.sait.samsung.co.kr

0167-2738/98/$ – see front matter
PII: S0167-2738(98)00174-X

In a recent publication, we reported on the cycling performances of rechargeable $Li/LiMn_2O_4$ cells which use acrylonitrile-methyl methacrylate-styrene (AMS)-based polymer electrolytes [11]. The ionic conductivity reaches an order of 1.0×10^{-3} S/cm in the AMS terpolymer-based polymer electrolyte containing $LiClO_4$-EC/PC at room temperature to give homogeneous films which exhibit good mechanical properties and electrochemical stability. However, $LiMn_2O_4$ showed a comparatively lower capacity, and most undesirably suffered a progressive capacity loss on cycling. Other materials such as $LiCoO_2$, $LiNiO_2$ and $LiNi_xCo_{1-x}O_2$ can be other cathode candidates. Among them, $LiNi_xCo_{1-x}O_2$ is known to have higher capacity and lower material cost than $LiCoO_2$. It also exhibits better thermal stability and rechargeability than $LiNiO_2$. Recently, we have synthesized $LiNi_{0.5}Co_{0.5}O_2$ powder by a sol-gel method using poly(acrylic acid) (PAA) as a chelating agent and studied its electrochemical performances for secondary lithium batteries [12]. This material exhibited a high capacity and good cycling behavior.

In this study, the polymer electrolytes composed of AMS terpolymer, liquid electrolyte, and silica powder have been prepared, and their electrochemical properties have been investigated. $LiNi_{0.5}Co_{0.5}O_2$ powder with uniform-sized particles were also synthesized by a sol-gel method using aspartic acid as a chelating agent. With these materials, we have assembled the $Li/SPE/LiNi_{0.5}Co_{0.5}O_2$ cells and investigated the electrochemical characteristics and cycling performance. The influence of mixed solvent electrolytes on charge-discharge cycling performance of the cell will be presented and discussed.

2. Experimental

2.1. Polymer synthesis

High-purity acrylonitrile (AN), methyl methacrylate (MMA) and styrene (ST) were purchased from Aldrich and used without further purification. AN-MMA-ST terpolymer (AMS) was synthesized via emulsion polymerization with distilled water at 60°C. Potassium persulfate ($K_2S_2O_8$) was used as a free-radical water-soluble initiator, and sodium lauryl sulfate was used as an emulsifier. The polymerization was continued for 6 h with vigorous agitation. The polymer was isolated by filtration and washed successively with distilled water at 80°C to remove any impurities such as residual monomers and initiator. The product was then dried in a vacuum oven at 100°C for 24 h. A white powder was obtained as a final product.

2.2. $LiNi_{0.5}Co_{0.5}O_2$ synthesis

A stoichiometric amount of Li, Ni and Co acetate salts with a molar ratio of Li:Ni:Co = 1:0.5:0.5 was dissolved in distilled water and completely mixed with an aqueous aspartic acid solution. The molar ratio of aspartic acid to the total metal ion content was 1.0. Nitric acid was slowly added to this solution with constant stirring until a pH of 4.0 was achieved. The resulting solution was then evaporated at 80°C for 4 h until a transparent sol was obtained. To remove water in the sol, it was further heated at 80°C while being stirred with a magnetic stirrer. As the evaporation of water proceeded, the sol turned into a viscous gel. The gel precursors obtained were calcined at 800°C for 10 h in air to obtain single-phase polycrystalline $LiNi_{0.5}Co_{0.5}O_2$ powders.

2.3. Characterization

^{1}H-NMR spectra were obtained in $CDCl_3$ on a Bruker-DRX-400 NMR spectrometer with tetramethylsilane (TMS) as an internal standard reference. Gel permeation chromatography (GPC) was carried out using a Waters CV-150 instrument equipped with three μ-Styragel columns (10^3, 10^4, 10^5 Å) and the system was calibrated with the monodisperse PS standards in THF. Powder X-ray diffraction using CuKα radiation was used to identify the crystalline phase of $LiNi_{0.5}Co_{0.5}O_2$ powders. The morphology of $LiNi_{0.5}Co_{0.5}O_2$ powder was examined using a scanning electron microscope (Jeol, JMS5800LV).

2.4. Preparation of polymer electrolytes

The AMS polymer was first dissolved in anhydrous THF. After the polymer was completely dissolved, a predetermined amount of liquid electrolyte

was added and the solution was further stirred. In the present study, we used two combinations of aprotic solvents: 1 M $LiClO_4$-EC/DMC (1:1 by vol.) and 1 M $LiClO_4$-EC/γ-BL (1:1 by vol.). EC was used as the principal solvent, since EC has a high dielectric constant which may be necessary to solvate the lithium salt. $LiClO_4$ was used as a salt because it forms highly conductive solutions with organic solvents and it has a high resistance to oxidation [13]. An appropriate amount of high-purity silanized fumed silica (Cabot Co.) was then added, which had been treated with hexamethyldisilazane. When complete homogenization of the mixture was achieved, the resulting viscous solution was cast with a doctor blade apparatus onto a release paper, then left to evaporate the solvent slowly at room temperature. After evaporation of THF, the film was separated from the release paper. The thickness of cast film was in the range of 80–200 μm. The polymer electrolyte was confirmed to be free of THF by means of ^{1}H-NMR. All procedures for preparing polymer electrolytes were carried out in a dry box filled with argon gas (99.999%).

2.5. Electrical measurements

Polymer electrolyte film was cut into 4 cm^2 squares and sandwiched between two stainless steel (SS) electrodes. In order to investigate the interfacial phenomena at the lithium electrode/polymer electrolyte interface, this sample was also sandwiched between the two lithium electrodes (Cyprus Foote Mineral Co., 50 μm thick). AC impedance measurement was then performed using a Zahner Elektrik IM6 impedance analyzer over the frequency range of 0.1 Hz–1 MHz with an amplitude of 10 mV.

2.6. Li/$LiNi_{0.5}Co_{0.5}O_2$ cell

A $LiNi_{0.5}Co_{0.5}O_2$ composite cathode on an aluminium foil consisted of $LiNi_{0.5}Co_{0.5}O_2$ with polymer electrolyte and super-P carbon in the proportions of 51:45:4 by weight percent. The anode consisted of 50-μm thick Li foil (Cyprus Foote Mineral Co.) pressed onto a Cu current collector. A rechargeable lithium polymer cell was assembled by sandwiching the polymer electrolyte between the lithium anode and the composite $LiNi_{0.5}Co_{0.5}O_2$ cathode. The cell was then enclosed in a metallized plastic bag and vacuum sealed. All assemblies of the cell were carried out in a dry box filled with argon gas. Cycle tests of lithium polymer cell were conducted in the voltage range of 3.0–4.2 V at different current densities with galvanostatically controlled equipment.

3. Results and discussion

The composition of the terpolymer was determined by ^{1}H-NMR spectrum, which is shown in Fig. 1. In the ^{1}H-NMR spectrum of AMS terpolymer, the methine protons in the benzene ring of the ST unit separately appear at $\delta = 7.00–7.19$ ppm and the methoxy protons of the MMA unit are observed at $\delta = 3.33–3.59$ ppm, whereas peaks of the methylene, methine and methyl protons in AN, MMA and ST units observed at higher field overlapped one another. The relative intensities of the methylene and methine protons in the ST unit could be calculated by multiplying the intensity of the methine proton in the benzene ring by 3/5. The intensities of the methylene and methyl protons in MMA could be also estimated by multiplying the intensity of the methoxy protons appearing at $\delta = 3.33–3.59$ ppm by 5/3. The intensities of the methylene and methine protons in AN are determined by subtracting the calculated intensities of the methylene, methine and methyl protons in ST and MMA from the total intensities of peaks superimposed at $\delta = 0.83–2.93$ ppm. The mole fraction of each monomer unit can thus be estimated by the total intensity of the corresponding monomer unit. The molar composition

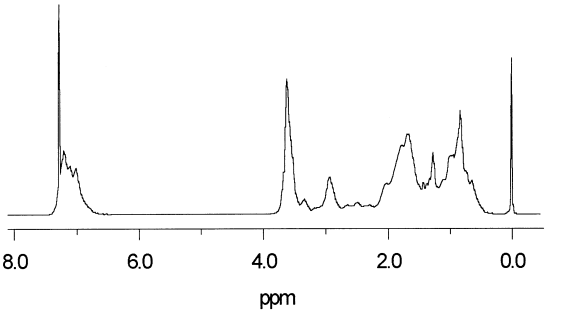

Fig. 1. ^{1}H-NMR spectrum of AMS terpolymer in $CDCl_3$ at 25°C.

of AN, MMA and ST was determined to be 55:29:16 from the ^{1}H-NMR spectrum shown in Fig. 1. From GPC analysis in THF, weight average molecular weight was determined to be 2 800 000 with a polydispersity index of 1.7.

The ionic conductivity and mechanical state of the polymer electrolytes prepared with AMS terpolymer and plasticizing liquid electrolyte were found to be dependent on the content of liquid electrolyte. To ensure high ionic conductivity of polymer electrolytes, the content of liquid electrolyte should be maintained to be higher than 80 wt.%. In the presence of 80 wt.% of liquid electrolyte, free standing and dimensionally stable thin films could be prepared. When the liquid electrolyte content was more than 85 wt.%, the polymer electrolytes became sticky and glutinous, and thus were difficult to handle. Thus, the amount of liquid electrolyte is maintained to be 80 wt.% in order to ensure high ionic conductivity and good mechanical stability. It is well known that the addition of inert filler is a useful tool to increase the electrical and mechanical properties of polymer electrolytes [14,15]. In our study, silanized fumed silica was added to a polymer electrolyte containing 20% AMS terpolymer and 80% liquid electrolyte. Silica is very fine dry powder with BET surface area of 212 m^2/g. The presence of the finely divided silica powder is shown to reinforce the physical strength of the film, such as tear strength. This reinforcement is related to the fact that the fine ceramic powder is homogeneously dispersed into a liquid electrolyte and forms a three-dimensional network which mechanically supports the solution. The influence of the silica powder content on the ionic conductivity is shown in Fig. 2. It is found that the EC/Y-BL system has shown higher conductivity than the EC/DMC electrolyte over the whole silica content range. Since the EC/Y-BL mixture has a high dielectric constant, it can form a gel with a considerable amount of carrier ions, which may result in an enhancement of ionic conductivity. It is also found that the ionic conductivity reaches a maximum around 10 wt.% of silica. An increase of conductivity with the addition of silica up to 10 wt.% is related to the enhancement of capacity to hold the liquid electrolyte, since the silanized fumed silica has a high adsorption capability, and subsequently enables loading of the plasticizing solvent. Over 10 wt.% of silica in the composite polymer electrolyte, the addition of silica powder decreases ionic conductivity due to the restriction of ionic motion. For the systems under study, the optimum filler content is thus believed to be 10% in terms of both ionic conductivity and mechanical stability.

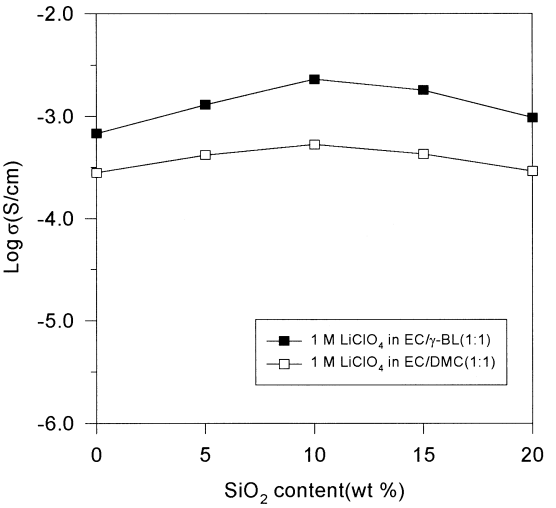

Fig. 2. Ionic conductivities with SiO_2 content for the AMS-based polymer electrolytes containing 80 wt.% of liquid electrolyte at 25°C.

In order to investigate the effect of solvent on the passivation phenomena of the lithium electrode, we examined the interfacial behavior of a lithium electrode in contact with polymer electrolytes containing different plasticizing solvents. Fig. 3 shows the time evolution of the ac impedance spectra of a Li/SPE/Li cell under open-circuit potential conditions at 25°C. In the literature [16–20], ac impedance response of the Li/SPE/Li cell has been treated in different ways, ranging from no deconvolution to a rather sophisticated one leading to the recognition of multi RC circuits corresponding to a multilayer structure of the surface film covering the Li electrode. It is out of the scope of this paper to analyze the nature and structure of the Li interface. Of particular interest in this investigation is a variation of the interfacial resistance, and thus we have considered a loop as a single semicircle and to follow only its time evolution. Fig. 4 shows the time evolution of the lithium interfacial resistance in the polymer electrolytes containing different solvent

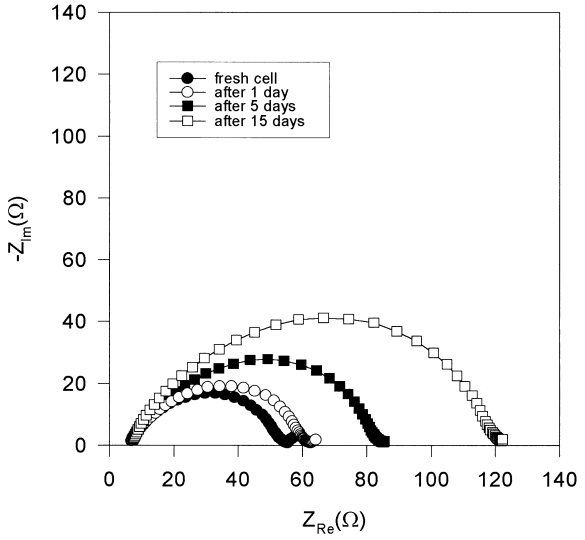

Fig. 3. AC impedance spectra of a Li/SPE/Li cell as a function of storage time at 25°C, where SPE consists of AMS (18 wt.%), 1 M $LiClO_4$ in EC/DMC (73 wt.%) and SiO_2 (9 wt.%).

mixtures. In Fig. 4, the interfacial resistance is seen to increase with storage time irrespective of polymer electrolytes examined. However the kinetics of passivation seem to be significantly different, suggesting a definite role of the solvent. In polymer electrolyte containing EC/Y-BL, the passivation occurs with a continuous growth and with a cumulative trend which becomes particularly dramatic as storage time increases. On the contrary, such a dramatic effect is not observed in the polymer electrolyte containing EC/DMC. The growth of the passivating film is related to the reactivity of the aprotic solvent with lithium metal. The surface chemistry of a lithium electrode in various solvent systems has been reported by many previous workers [21–24]. In the case of alkyl carbonate such as EC, DMC, the major surface species formed on the lithium electrode are lithium alkyl carbonate (ROCOOLi) as the product of one electron reduction process of the solvent in the presence of Li^+, which was known to be a good passivating agent [21,23]. On the other hand, the lithium/Y-BL system is quite reactive, and surface films formed on lithium in Y-BL contains mostly lithium butyrate and lithium salt of a cyclic β-keto ester anion, as Aurbach has previously reported [22]. These previous results suggest a strong involvement of solvent in the build-up of the surface film and reflect the different degree of reactivity of the various solvents with the lithium electrode. From the results in Fig. 4, EC/DMC mixture is thought to be a preferred system in terms of the long term stability of the passivation layer of a lithium electrode. Therefore, one may expect that the extent of the passivation can be limited to such an extent to assure acceptable stability of the interface by the selection of a proper solvent.

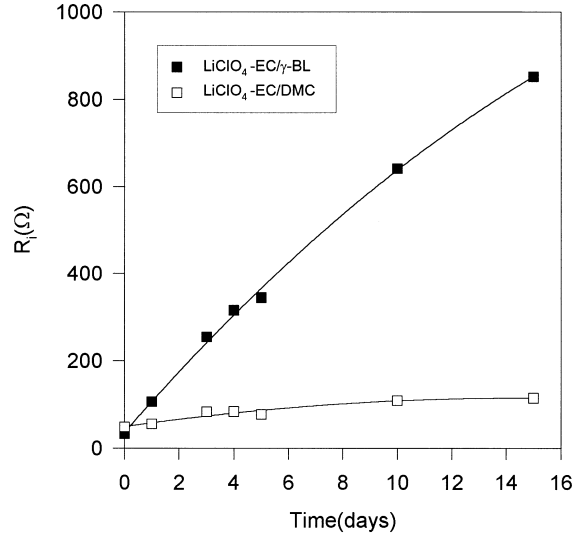

Fig. 4. Variation of interfacial resistances with storage time in the Li/SPE/Li cell with polymer electrolytes containing different solvent mixtures.

Fig. 5 shows the X-ray diffraction (XRD) pattern for the $LiNi_{0.5}Co_{0.5}O_2$ powder. It was confirmed

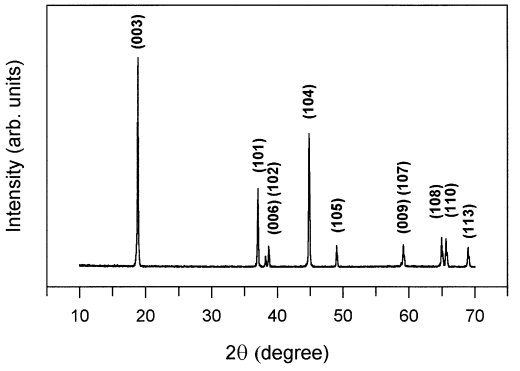

Fig. 5. X-ray diffraction pattern of the $LiNi_{0.5}Co_{0.5}O_2$ powder.

from the XRD pattern that phase-pure $LiNi_{0.5}Co_{0.5}O_2$ was obtained, and all diffraction peaks could be indexed by assuming the structure to be a hexagonal lattice of an α-$NaFeO_2$ type. In the case of $LiNiO_2$ or $LiNi_{1-x}Co_xO_2$ phases, the nickel ions in the lithium layer block the lithium ion diffusion path. It has been reported that the changes in layer occupancy have a direct effect on the XRD patterns such as the integrated intensity ratios I(003)/I(104) and I(006,102)/I(101), and the split of the (108) and (110) lines [25,26]. When the integrated intensity ratio of (003) to (104) peaks was below 1.2, either the (108) and (110) peaks, or (006) and (102) peaks, become difficult to distinguish from each other. Disorder of this nature which is called cation mixing between Li and Co or Ni cations can seriously degrade electrochemical performance of the cathode such as rechargeable capacity and cyclability. It is seen from the figure that the observed value of integrated intensity ratio of I(003)/I(104) is 1.24 and the lines of (102) and (006), and (108) and (110) are clearly split. Since the cross-linked gel precursors may provide more homogeneous mixing of the cations and less tendency for segregation during calcination, the use of aspartic acid as a chelating agent in preparing $LiNi_{0.5}Co_{0.5}O_2$ by sol-gel process greatly suppresses the formation of precipitates from which the heterogeneity stems. Fig. 6 shows the scanning electron micrograph of the $LiNi_{0.5}Co_{0.5}O_2$ powder. It was observed that the particle size of the particulates was about 3 μm with a fairly narrow particle-size distribution.

We fabricated the $Li/SPE/LiNi_{0.5}Co_{0.5}O_2$ cells using the AMS-based polymer electrolytes and $LiNi_{0.5}Co_{0.5}O_2$ composite cathode. Fig. 7 shows the first charge-discharge curve for $Li/SPE/LiNi_{0.5}Co_{0.5}O_2$ cell with polymer electrolyte containing EC/DMC mixture as a plasticizing solvent, at a constant current density of 0.1 mA/cm^2. This $Li/SPE/LiNi_{0.5}Co_{0.5}O_2$ cell has a first charge capacity of 162 mAh/g followed by reversible discharge capacity of 156 mAh/g. The initial coulombic efficiency of this cell was about 96.3%. Table 1 summarizes the electrochemical performance of the $Li/SPE/LiNi_{0.5}Co_{0.5}O_2$ cell with polymer electrolytes containing EC/DMC and EC/γ-BL. It is found that the initial coulombic efficiency of the $Li/SPE/LiNi_{0.5}Co_{0.5}O_2$ cell is almost the same, regardless of solvent used. However the discharge capacity of the cell is higher in EC/γ-BL than in EC/DMC, which may be caused by lower electrolyte resistance of the EC/γ-BL system. Fig. 8 shows the charge-discharge curves with number of cycles for $Li/SPE/LiNi_{0.5}Co_{0.5}O_2$ cell with polymer electrolyte containing EC/DMC mixture, and Fig. 9 shows the discharge capacities as a function of cycle number in the $Li/SPE/LiNi_{0.5}Co_{0.5}O_2$ cell with polymer electrolytes containing different liquid electrolyte. Fig. 9 clearly shows that cycling performance

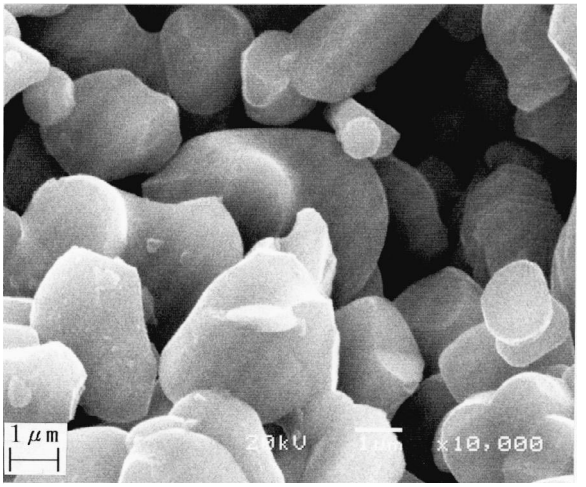

Fig. 6. Scanning electron micrograph of the $LiNi_{0.5}Co_{0.5}O_2$ powder.

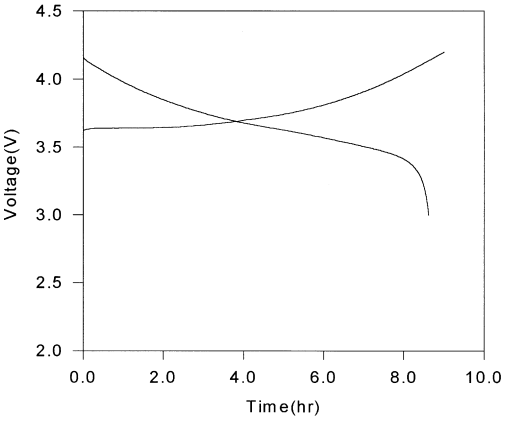

Fig. 7. First charge-discharge curve for $Li/SPE/LiNi_{0.5}Co_{0.5}O_2$ cell with polymer electrolyte containing EC/DMC mixture at a constant current density of 0.1 mA/cm^2.

Table 1
Electrochemical performance of Li/SPE/$LiNi_{0.5}Co_{0.5}O_2$ cells with polymer electrolytes containing different solvents

Solvent	EC/DMC	BC/Y-BL
1st charge capacity (mAh/g)	162	167
1st discharge capacity (mAh/g)	156	160
Coulombic efficiency for the 1st cycle (%)	96.3	95.9

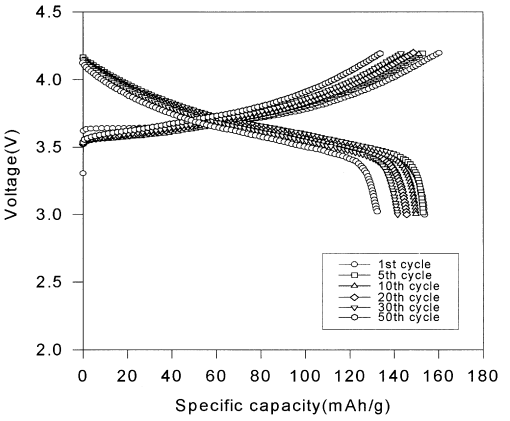

Fig. 8. Cycling curves of Li/SPE/$LiNi_{0.5}Co_{0.5}O_2$ cell containing EC/DMC at 0.1 mA/cm^2 (0.1 C rate).

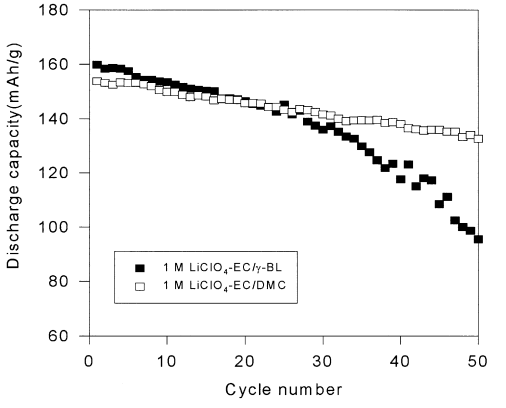

Fig. 9. Discharge capacities of the Li/SPE/$LiNi_{0.5}Co_{0.5}O_2$ cell as a function of cycle number at 0.1 mA/cm^2 (0.1 C rate).

of Li/SPE/$LiNi_{0.5}Co_{0.5}O_2$ cell depends on the solvent mixture used. The use of EC/DMC-based polymer electrolytes allows better cycling characteristics to be reached, while very poor cycling characteristics are observed in Li/SPE/$LiNi_{0.5}Co_{0.5}O_2$ cell with polymer electrolyte containing EC/Y-BL mixture. The cycling characteristics of the Li/SPE/$LiNi_{0.5}Co_{0.5}O_2$ cell is expected to be influenced by the dynamics of Li passivation and other factors such as the deterioration of interfacial contacts for composite cathode ($LiNi_{0.5}Co_{0.5}O_2$/conducting carbon/polymer electrolyte). If there is little dependence of solvent mixture on the morphology of composite cathode during charge-discharge cycling, one might speculate that the Li/SPE interface plays an important role in determining the cell behavior in terms of cyclability for Li/SPE/$LiNi_{0.5}Co_{0.5}O_2$ cell. As shown in Fig. 4, the interfacial resistance of Li/SPE abruptly increases and reaches the higher value in the polymer electrolyte containing EC/Y-BL, which may influence the plating-stripping cycles of lithium, and leads to a large capacity fading of the Li/SPE/$LiNi_{0.5}Co_{0.5}O_2$ cell.

The study of the nature of electrolyte/electrode interface is expected to give a direct relevance to the understanding of the cycling characteristics of the lithium polymer cell. Fig. 10 and Fig. 11 show the ac impedance spectra of the Li/SPE/$LiNi_{0.5}Co_{0.5}O_2$ cells with polymer electrolytes containing EC/DMC and EC/Y-BL, respectively, at fully discharged state. For the freshly made cell, only one arc appeared so the equivalent circuit comprises the electrolyte resistance R_e and the total interface resistance. After one charge/discharge cycling, the spectrum showed two arcs. The first one observed at middle frequency may be related to the Li/electrolyte interface (R_a), and the second one appeared at low frequency to the cathode/electrolyte interface (R_c), as previously reported by Selvaggi et al. [27]. This presumption was confirmed by the fact that a new semicircle related to the cathode/electrolyte interface can be observed after the first charge/discharge cycle. This behavior can be ascribed to an initial poor interfacial contact between electrolyte/cathode before charge/discharge cycling, which means that current flow is necessary to activate an initially poor electrolyte/cathode interface. Table 2 lists the electrolyte resist-

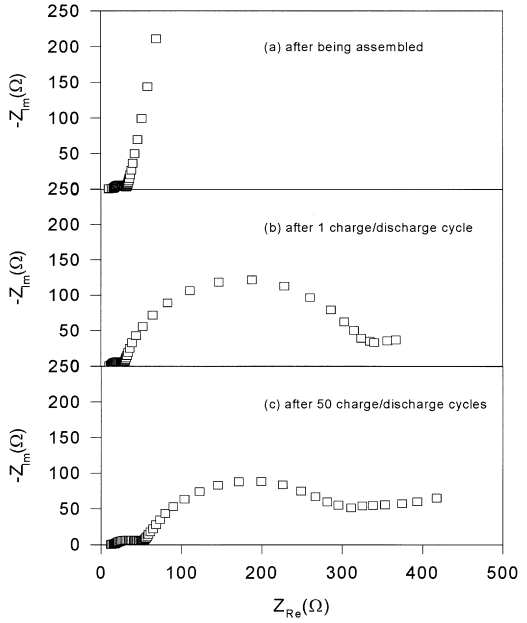

Fig. 10. AC impedance spectra of $Li/SPE/LiNi_{0.5}Co_{0.5}O_2$ cell with polymer electrolyte containing EC/DMC at fully discharged state; (a) after being assembled, (b) after one charge/discharge cycle, (c) after 50 charge/discharge cycles.

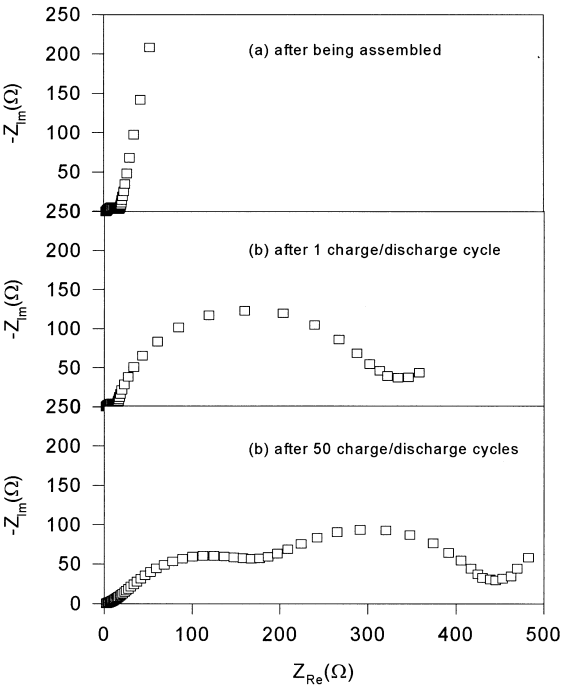

Fig. 11. AC impedance spectra of $Li/SPE/LiNi_{0.5}Co_{0.5}O_2$ cell with polymer electrolyte EC/Y-BL at fully discharged state; (a) after being assembled, (b) after one charge/discharge cycle, (c) after 50 charge/discharge cycles.

ance (R_e) and the interfacial resistances (R_a and R_c) obtained from ac impedance spectra given in Fig. 10 and Fig. 11. It should be noted that the interfacial resistance assigned to the Li/electrolyte interface becomes much larger after 50 charge/discharge cycles in the $Li/SPE/LiNi_{0.5}Co_{0.5}O_2$ cell with polymer electrolyte containing EC/Y-BL. This result is due to the fact the corrosion of the lithium electrode in EC/Y-BL-based polymer electrolyte is enough to increase the interfacial resistance, as explained in Fig. 4. On the other hand, the interfacial characteristics of cathode/electrolyte can be regarded as good, because the interfacial resistance related to the cathode/electrolyte decreased after 50 cycles in both electrolyte systems. This is a convincing indication of a good interfacial contact in composite cathode, thus, capacity loss on cycling due to the degradation of positive interface can be considered negligible in our systems. From these results, it can be said that the progressive decline in capacity in $Li/SPE/LiNi_{0.5}Co_{0.5}O_2$ cells with EC/Y-BL-based polymer electrolyte as compared to those with EC/DMC-based polymer electrolyte is related to the higher interfacial resistance between Li and electrolyte interface due to the passive layer formed at the lithium electrode. Although EC/Y-BL-based polymer electrolyte exhibits higher ionic conductivity (2.3×10^{-3} S/cm) than EC/DMC-based polymer electrolyte (5.3×10^{-4} S/cm), the poor interfacial properties between lithium and electrolyte limit cycling performance of the $Li/SPE/LiNi_{0.5}Co_{0.5}O_2$ cell, which indicates that the criteria for the selection of a proper polymer electrolyte system should be based not only on fast ion transport properties but also on favorable interfacial characteristics.

Cycling results of $Li/SPE/LiNi_{0.5}Co_{0.5}O_2$ cells with EC/DMC-based polymer electrolyte is superior to those based on EC/Y-BL. With these polymer electrolytes, we tried to obtain the rate capability of $Li/SPE/LiNi_{0.5}Co_{0.5}O_2$ cells. Fig. 12 represents the discharge curves of the $Li/SPE/LiNi_{0.5}Co_{0.5}O_2$ cells obtained at different current rates. The cell delivered a capacity of 155 mAh/g at 0.2 C rate. It is found that the polarization was increased as the current rate

Table 2
Electrolyte (R_e) and interfacial resistances (R_a and R_c) of Li/SPE/$LiNi_{0.5}Co_{0.5}O_2$ cells with polymer electrolytes containing different solvents

Mixed solvent	EC/DMC			EC/Y-BL		
Resistance	Fresh cell	After one cycle	After 50 cycles	Fresh cell	After one cycle	After 50 cycles
R_e (Ω)	8.9	9.2	10.4	2.1	2.2	2.2
R_a (Ω)	21.3	17.8	37.1	14.5	11.4	165.0
R_c (Ω)	–	322.3	261.5	–	320.3	277.8

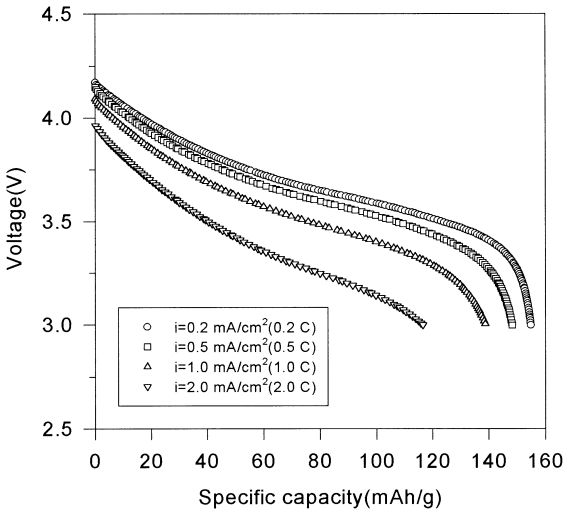

Fig. 12. Discharge curves of Li/SPE/$LiNi_{0.5}Co_{0.5}O_2$ cell with polymer electrolyte containing EC/DMC at different current rates.

increased, which results in the decrease of capacity. However, it showed the attractive capacity of 116 mAh/g at 2.0 C rate, which was 75% of discharge capacity at 0.2 C rate. From the results described above, it is expected that the Li/SPE/$LiNi_{0.5}Co_{0.5}O_2$ cells with AMS-based polymer electrolytes containing plasticizing solvents compatible with the Li electrode are promising candidates for a Li secondary battery with high energy density and rate capability.

4. Conclusion

Novel free standing gel polymer electrolytes based on acrylonitrile-methyl methacrylate styrene terpolymer were prepared using binary plasticizing solvents consisting of EC/DMC or EC/Y-BL. The rechargeability of the Li/SPE/$LiNi_{0.5}Co_{0.5}O_2$ cells containing EC/DMC showed better cycling characteristics than those containing EC/Y-BL. The nature of the solvent affected the cyclability of Li/SPE/$LiNi_{0.5}Co_{0.5}O_2$ cells, and thus, lithium polymer batteries with better cycle life and efficient rechargeability are expected to be possible with polymer electrolytes containing solvents compatible with the Li electrode. The Li/SPE/$LiNi_{0.5}Co_{0.5}O_2$ cell based on the EC/DMC mixture had an initial capacity of 156 mAh/g in the voltage range of 3.0–4.2 V. It also showed the attractive discharge capacity of 116 mAh/g at 2.0 C rate.

References

[1] M. Watanabe, M. Kanba, K. Nagaoka, I. Shinohara, J. Polym. Sci. Polym. Phys. Ed. 21 (1983) 939.
[2] F. Croce, F. Gerace, G. Dautzemberg, S. Passerini, G.B. Appetecchi, B. Scrosati, Electrochim. Acta 39 (1994) 2187.
[3] D. Peramunage, D.M. Pasquariello, K.M. Abraham, J. Electrochem. Soc. 142 (1995) 1789.
[4] K. Tsunemi, H. Ohno, E. Tsuchida, Electrochim. Acta 28 (1983) 591.
[5] K. Tsunemi, H. Ohno, E. Tsuchida, Electrochim. Acta 28 (1983) 833.
[6] M. Alamgir, K.M. Abraham, J. Electrochem. Soc. 140 (1993) L96.
[7] S. Passerini, J.M. Rosolen, B. Scrosati, J. Power Source 45 (1993) 333.
[8] K.M. Abraham, M. Alamgir, J. Electrochem. Soc. 137 (1990) 1657.
[9] D.W. Kim, Y.R. Kim, J.K. Park, S.I. Moon, Solid State Ionics 106 (1998) 329.
[10] D.W. Kim, Y.R. Kim, Y.K. Sun, B.K. Oh, B.S. Jin, S.I. Moon, Polymer (Korea) 21 (1997) 861.
[11] D.W. Kim, Y.R. Kim, Y.K. Sun, S.E. Kang, International Meeting of the Electrochemical Society and the International Society of Electrochemistry, Paris, France, Aug 31–Sept 5, 1997, Abstract no. 199.

[12] Y.K. Sun, I.H. Oh, K.Y. Kim, J. Mater. Chem. 7 (1997) 1481.
[13] J.M. Tarascon, D. Guyomard, Solid State Ionics 69 (1994) 293.
[14] J.B. Weston, B.C.J. Steele, Solid State Ionics 7 (1982) 75.
[15] J. Fan, P.S. Fedkiw, J. Electrochem. Soc. 144 (1997) 399.
[16] N. Takami, T. Ohsaki, K. Inada, J. Electrochem. Soc. 139 (1992) 1849.
[17] J.G. Thevenin, R.H. Muller, J. Electrochem. Soc. 134 (1987) 273.
[18] G. Nagasubramanian, A.I. Attia, G. Halpert, J. Appl. Electrochem. 24 (1994) 298.
[19] A. Zaban, D. Aurbach, J. Power Source 54 (1995) 289.
[20] D.W. Kim, J.K. Park, J.S. Bae, S.I. Pyun, J. Polym. Sci. Polym. Phys. Ed. 34 (1996) 2127.
[21] D. Aurbach, H.E. Gottlieb, Electrochim. Acta 34 (1989) 141.
[22] D. Aurbach, J. Electrochem. Soc. 136 (1989) 1606.
[23] D. Aurbach, Y. Gofer, M. Ben-Zion, P. Aped, J. Electroanal. Chem. 339 (1992) 451.
[24] D. Aurbach, I. Weissman, A. Zaban, O. Chusid, Electrochim. Acta 39 (1993) 51.
[25] T. Ohzuku, H. Komori, M. Nagayama, K. Sawai, T. Hirai, J. Ceram. Soc. Jpn. 100 (1992) 346.
[26] J.R. Dahn, U. von Sacken, C.A. Michal, Solid State Ionics 44 (1990) 87.
[27] A. Selvaggi, F. Croce, B. Scrosati, J. Power Source 32 (1990) 389.